Cleaning lateral morphological features of the root canal

Robinson, J P; Macedo, R G; Verhaagen, B; Versluis, M; Cooper, P R; van der Sluis, Lucas; Walmsley, A D

Published in:
International Endodontic Journal

DOI:
10.1111/iej.12804

INTERNATIONAL
ENDODONTIC JOURNAL

doi:10.1111/iej.12804

Cleaning lateral morphological features of the root canal: the role of streaming and cavitation

J. P. Robinson[1,*], R. G. Macedo[2,*], B. Verhaagen[3], M. Versluis[3], P. R. Cooper[4], L. W. M. van der Sluis[5] & A. D. Walmsley[4]

[1]Physical Sciences of Imaging in the Biomedical Sciences, University of Birmingham, Birmingham, UK; [2]Department of Cariology, Endodontology & Pedodontology, ACTA Academic Center for Dentistry Amsterdam, University of Amsterdam and VU University, Amsterdam; [3]Physics of Fluids group and MIRA Institute for Biomedical Technology and Technical Medicine and MESA + Institute for Nanotechnology, University of Twente, Enschede, The Netherlands; [4]School of Dentistry, Institute of Clinical Sciences, University of Birmingham, Birmingham, UK; and [5]Center for Dentistry and Oral Hygiene, University Medical Center Groningen, Groningen, The Netherlands

Abstract

Robinson JP, Macedo RG, Verhaagen B, Versluis M, Cooper PR, van der Sluis LWM, Walmsley AD. Cleaning lateral morphological features of the root canal: the role of streaming and cavitation. *International Endodontic Journal*, **51**, e55–e64, 2018.

Aim To investigate the effects of ultrasonic activation file type, lateral canal location and irrigant on the removal of a biofilm-mimicking hydrogel from a fabricated lateral canal. Additionally, the amount of cavitation and streaming was quantified for these parameters.

Methodology An intracanal sonochemical dosimetry method was used to quantify the cavitation generated by an IrriSafe 25 mm length, size 25 file inside a root canal model filled with filtered degassed/saturated water or three different concentrations of NaOCl. Removal of a hydrogel, demonstrated previously to be an appropriate biofilm mimic, was recorded to measure the lateral canal cleaning rate from two different instruments (IrriSafe 25 mm length, size 25 and *K* 21 mm length, size 15) activated with a P5 Suprasson (Satelec) at power P8.5 in degassed/saturated water or NaOCl. Removal rates were compared for significant differences using nonparametric Kruskal–Wallis and/or Mann–Whitney *U*-tests. Streaming was measured using high-speed particle imaging velocimetry at 250 kfps, analysing both the oscillatory and steady flow inside the lateral canals.

Results There was no significant difference in amount of cavitation between tap water and oversaturated water ($P = 0.538$), although more cavitation was observed than in degassed water. The highest cavitation signal was generated with NaOCl solutions (1.0%, 4.5%, 9.0%) ($P < 0.007$) and increased with concentration ($P < 0.014$). The IrriSafe file outperformed significantly the *K*-file in removing hydrogel ($P < 0.05$). Up to 64% of the total hydrogel volume was removed after 20 s. The IrriSafe file typically outperformed the *K*-file in generating streaming. The oscillatory velocities were higher inside the lateral canal 3 mm compared to 6 mm from WL and were higher for NaOCl than for saturated water, which in turn was higher than for degassed water.

Conclusions Measurements of cavitation and acoustic streaming have provided insight into their contribution to cleaning. Significant differences in cleaning, cavitation and streaming were found depending on the file type and size, lateral canal location and irrigant used. In general, the IrriSafe file outperformed the *K*-file, and NaOCl performed better than the other irrigants tested. The cavitation and streaming measurements revealed that both contributed to hydrogel removal and both play a significant role in root canal cleaning.

Keywords: cavitation, cleaning, lateral canal, streaming.

Received 31 January 2017; accepted 19 June 2017

Correspondence: Michel Versluis, Physics of Fluids group and MIRA Institute for Biomedical Technology and Technical Medicine and MESA+ Institute for Nanotechnology, University of Twente, P.O. 217, 7500AE Enschede, The Netherlands (e-mail: m.versluis@utwente.nl).

*Both authors contributed equally to this study and should both be listed as first author

Introduction

The aim of root canal treatment is to remove bacterial biofilm from an infected canal. Any remaining microorganisms have the potential to re-establish a biofilm in the canal (Busscher *et al.* 2010, Ohsumi *et al.* 2015). The biofilm is an agglomeration of bacteria, adhered to a surface and embedded in a self-produced extracellular polymeric substance (EPS). This EPS matrix provides the biofilm with viscoelastic properties, facilitates nutrition and protects it from chemical and mechanical attacks imposed by endodontic cleaning procedures and disinfectants (de Paz 2007, Stewart & Franklin 2008). The viscoelastic properties of the EPS matrix also facilitate the biofilm's ability to deform and adapt under mechanical stress (Körstgens *et al.* 2001)

Inside a root canal, this infecting biofilm is particularly problematic and difficult to remove, especially when it forms in the accessory root canal system such as in lateral canals, which communicate with the surrounding bone. Persistent infection in such confined areas, unreachable by files during root canal preparation (Peters *et al.* 2001), is a common cause of root canal treatment failure (Wu & Wesselink 2005, Ricucci *et al.* 2013).

Biofilm removal has been attempted using syringe irrigation, laser irrigation and ultrasonic activation (van der Sluis *et al.* 2015). The latter, Ultrasonic Activated Irrigation (UAI), makes use of ultrasonically oscillating files with the aim of improving the chemical and mechanical efficacy of root canal cleaning. In UAI, both cavitation and microstreaming occur even at the lowest clinically significant power settings, in addition their occurrence increases proportional to the ultrasonic power (Macedo *et al.* 2014a,b). The amount of cavitation is dependent on the instrument design, tip size and taper, and also on the type of irrigant and on the confinement of the file within the canal (Macedo *et al.* 2014a,b). Transient cavitation (growth and subsequent implosion of bubbles) has been found both in straight and curved canals, at the entrance of simulated lateral canals and isthmi, and up to 2 mm beyond the tip of the file (Macedo *et al.* 2014b).

Few studies have thus far focused on how the biofilm as a structure responds to mechanical stress. A hydrogel mimicking the viscoelastic properties of a biofilm has been reported (Macedo *et al.* 2014c). Visualization of the removal of a hydrogel from lateral canal anatomies by UAI indicated that microstreaming and transient cavitation may be critical to biofilm cleaning efficacy; however, their central contribution in the cleaning process has not yet been evaluated. Understanding this behaviour in relation to flow and related fluid dynamical phenomena, for example cavitation, is fundamental for optimizing biofilm removal strategies in root canal cleaning.

The aim of this study, therefore, was to investigate the effects of file type, lateral canal location and irrigant on the removal of hydrogel from a lateral canal. In addition, the amount of cavitation and streaming was quantified for these parameters. The null hypothesis was that all file types/irrigant combinations performed equally and that lateral canal location did not affect cleaning efficacy.

Materials & methods

Cavitation quantification by sonochemical dosimetry

A previously described intracanal sonochemical dosimetry method (Macedo *et al.* 2014a) was used to measure sonoluminescence (SL) generated by the endodontic files. The SL signal gave a direct measure of the amount of transient cavitation occurring around an endodontic file. The endodontic file was positioned in a PDMS (PolyDiMethylSiloxane; Sylgard 184, Dow-Corning, Midland, MI, USA) root canal model. The canal has an apical diameter of 0.45 mm, a taper of 6% and a length of 20 mm and was fixed inside a $1.0 \times 1.0 \times 4.0\ cm^3$ cuvette (Plastibrand, Brand, Wertheim, Germany).

The Ultrasonic Activated Irrigation was performed with 25 mm long, size 25 IrriSafe files (Satelec Acteon, Merignac, France), driven with a commercial endodontic ultrasound device (P-Max, Satelec Acteon) at its maximum power 'Red 10'. The instruments were centred and fixed 1 mm from working length (WL). The ultrasound device was driven by a pulse generator (TGP110, TTi, Huntingdon, UK) in 18 series for a period of 10 s with a duty cycle of 30%, consisting of 3 s ON and 7 s OFF. After each three series of measurements, the file and irrigant were replaced and none of the files fracture during the experiments.

Six irrigants were included in the measurements: (i) Filtered water (Millipore Corporation, Billerica, MA, USA); (ii) Degassed filtered water which had been degassed using a vacuum pump for a minimum of 30 min; (iii) Oversaturated filtered water obtained by pumping air into filtered water for at least 30 min;

(iv) 1% NaOCl solution (Sigma-Aldrich, St. Louis, MO, USA); (v) 4.5% NaOCl solution; (vi) 9% NaOCl Solution. NaOCl solutions were obtained by dilution of a 10%–15% NaOCl (Sigma-Aldrich) with filtered water. Each measurement was repeated three times. The concentration of the various NaOCl solutions was measured immediately prior to starting the experiments using a standard titration method (Vogel 1962).

To measure the SL intensity, a photomultiplier tube (PMT; R508, Hamamatsu Photonics, Hamamatsu, Japan) was mounted within a light-tight box and adjacent to the cuvette containing the root canal model. The PMT received an electrical voltage of 1.6 kV from a DC power supply (6516A, Hewlett-Packard, Palo Alto, CA, USA). Its output was recorded at a rate of 300 kHz with a high-speed data acquisition device (DAQ; USB-6356, National Instruments, Austin, TX, USA). The average and standard deviation of each of the 18 measurements were calculated as previously described (Macedo *et al.* 2014a). A calibration measurement demonstrated that there was a linear response of the PMT up to an output voltage of 1 V and an interclass correlation coefficient score of 0.994 for single measurements with $P < 0.001$ was obtained.

Hydrogel removal from a lateral canal

A second set of transparent root canal models included lateral canals, as described before for the investigation of root canal cleaning (Macedo *et al.* 2014c). The models exhibited the very same dimensions as the one described above, but with a lateral canal with a diameter of 200 μm and positioned 3 mm or 6 mm from the apex.

A hydrogel, demonstrated previously to be an appropriate biofilm mimic, was prepared as described (Macedo *et al.* 2014a). Prior to being used, it was stored in an oven at 30 °C (Hybridization oven S1 20H, Stuart Scientific, Stone, UK). The viscoelastic properties were confirmed to be similar to those described by Macedo *et al.* (2014a).

The hydrogel was placed in the lateral canal using a 30G needle (Becton, Dickson and Company, Oxford, UK) and remained there for at least 1 min to cool and solidify at room temperature. After that, the root canal was filled with irrigant. The ultrasonic file was positioned in the centre of the model with the file tip aligned to the entrance of the lateral canal, and the oscillation direction was in plane with the lateral canal. The file was driven by an ultrasonic device (P5 Suprasson, Satelec Acteon) at a power setting of 8.5/20 (42.5%), corresponding with a power setting of 'Yellow 5' as used in a previous study (Macedo *et al.* 2014a).

The root canal models were imaged using a bright-field microscope (Leitz Dialux 22, Leica, Wetzlar, Germany) and a digital SLR camera equipped with a 12.3 megapixel CMOS sensor (D5000, Nikon, Tokyo, Japan) at a recording rate of 24 fps. The sample was magnified by a 10× objective, resulting in 900 μm of the lateral canal visible in the recordings, which corresponds to a hydrogel volume of 28 nL.

The experiment was performed using two instruments (IrriSafe length 25 mm, size 25 and length 21 mm, size 15 Satelec Acteon) and three irrigants ($n = 10$) resulting in six experimental groups. Activation was performed for 20 s, following the recommended UAI protocol (van der Sluis *et al.* 2010, Macedo *et al.* 2014d). Studies were undertaken on a lateral canal positioned 6 mm from the apex. The irrigants studied included saturated water, degassed water and sodium hypochlorite (NaOCl, Septodont, Maidstone, UK). Saturated water was prepared by pumping air into filtered water for at least 30 min; degassed water was prepared by placing filtered water in a vacuum chamber for at least 30 min. Filtered water was prepared by running tap water through carbon, 5 μm sediment and DI filters (Osmotics, Aylsham, UK). NaOCl was determined to have a concentration of 4.5% by a standard titration protocol (Vogel 1962).

An additional study ($n = 5$) was performed using the two instruments on a lateral canal located 3 mm from the apex. Both saturated and degassed water were compared resulting in four experimental groups.

In a control group, NaOCl was used as irrigant in the absence of UAI, to study the chemical reaction between NaOCl and the hydrogel.

The area occupied by the hydrogel was calculated into volume for each frame of the videos using a MATLAB script (The MathWorks, Natick, MA, USA). Mean and average volume were calculated for each group and plotted as a function of time.

Nonparametric Kruskal–Wallis with Mann–Whitney U as *post hoc* tests were performed to compare the volume of hydrogel removed, for each root canal model, and for the three different irrigation solutions (degassed and saturated filtered water and 4.5% NaOCl solution). Mann–Whitney *U*-tests were used to compare the volume of hydrogel removal in lateral

canals at two positions (3 vs. 6 mm), by two file types (IS length 25 mm, size 25 and *K* length 21 mm, size 15,) and between activated and nonactivated irrigation with NaOCl at 4.5%. For all tests, *P*-values < 0.05 were considered statistically significant. The statistical values were calculated for 1–10 and 11–20 s of hydrogel removal.

Velocity measurements with particle imaging velocimetry (PIV)

The streaming around an unconfined endodontic file was recorded using a high-speed camera (HPV-1, Shimadzu Corp., Kyoto, Japan), capable of recording 100 frames at speeds up to 10^6 frames s^{-1}. The camera was attached to a microscope (Leitz Dialux 22, Leica) with a 20 × magnification objective, with a measurement depth of field of 100 μm. Illumination for bright-field imaging was provided by a continuous wave light source (KL2500, Schott, Germany).

An IrriSafe length 25 mm, size 25 or *K* length 21 mm, size 15 file was positioned inside the PDMS root canal models described above, filled with degassed or saturated demi water, or with a NaOCl solution (4.5%). The file tip was aligned with the lateral canal entrance. Activation was performed using an ultrasound device (P5 Suprasson, Satelec Acteon) operated at a power setting of 8.5/20. Monodisperse hollow glass spheres of diameter 10 μm (Sphericel, Potters Industries, Barnsley, UK; mean density of $1.1 \cdot 10^3$ kg m^{-3}, Stokes number *O* (1) for the highest velocities occurring indicating that they follow the flow well) were added to the liquids.

The flow was analysed from the high-speed recordings using a particle imaging velocimetry algorithm developed in-house (Verhaagen *et al.* 2013a). The oscillatory component was analysed by calculating the ensemble average over 2–3 frames for each area of 16 × 16 pixels down the lateral canal. The resulting velocity vs. distance plots were verified to show translatory oscillations of approx. 30 kHz; the rms value was used as final value for the oscillatory velocity, whilst the steady component of the velocity was calculated from the mean of the velocimetry result.

Measurements were performed ten times for each file and each liquid. Due to the large range of the velocities (which could not be captured in a single video), videos were made at two recording speeds: at 250 kfps, for the oscillatory component, and at 63 kfps, for the steady component.

Results

Hydrogel removal

The hydrogel located in the lateral canal detached in fragments. Figure 1 shows the hydrogel removal as a function of time, averaged over the 10 repeated experiments.

For a lateral canal at 6 mm, the greatest removal rate occurred with NaOCl, followed by saturated and then degassed water (Fig. 1). The differences between the three irrigants after 20 s were significant for the IrriSafe file ($P < 0.05$, Fig. 1b), at which moment 28/43/64% was removed for degassed and saturated water and NaOCl, respectively. For the *K*-file, only degassed water and NaOCl were significantly different ($P < 0.05$, Fig. 1a). In the absence of activation, the removal of hydrogel by the chemical reaction between

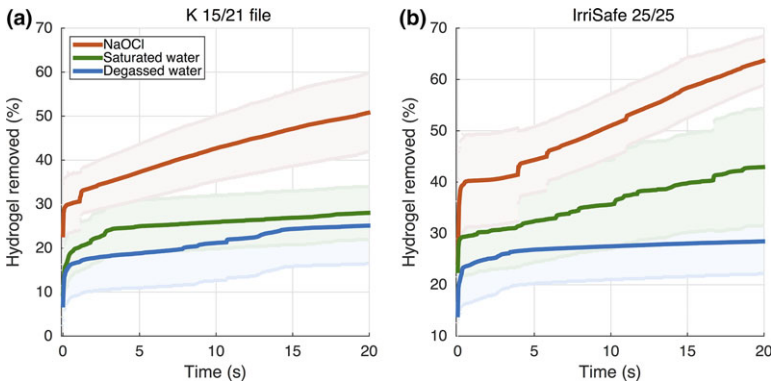

Figure 1 Hydrogel removal (percentage of hydrogel that was visible) versus time, for the *K*-file (a) and IrriSafe file (b), for three different liquids. Lateral canal at 6 mm from WL. The plots show the means (solid lines) and standard deviations (typically 10% of the mean; indicated with shaded areas).

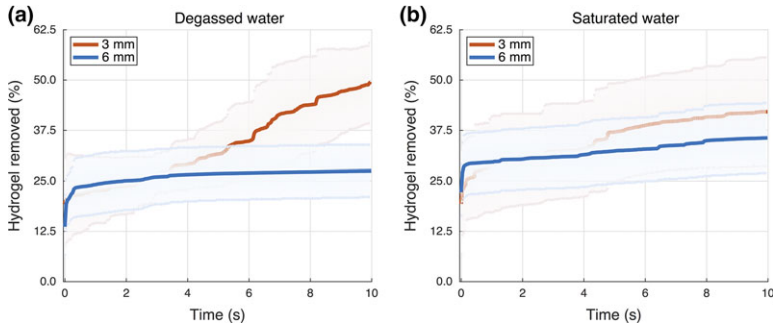

Figure 2 Hydrogel removal versus time for degassed and saturated water, comparing the lateral canal at 3 or 6 mm from WL.

NaOCl and the hydrogel occurred at a much lower rate ($P < 0.001$).

The IrriSafe file outperformed the *K*-file in the lateral canal positioned at 6 mm, removing more hydrogel with NaOCl ($P < 0.05$) and saturated water ($P < 0.01$) in 20 s (Fig. 1) (43% and 28%, respectively, for saturated water). When averaging all irrigants for this lateral canal, the difference between the two file types was highly significant ($P = 0.001$).

There were no significant differences between degassed and saturated water in a lateral canal positioned at 3 mm (Fig. 2a,b). With the lateral canal at 3 mm vs. 6 mm, more hydrogel was removed (49% and 27%, respectively, after 20 s with degassed water), although this difference was not always significant.

In many of the recordings involving saturated water and NaOCl, small transient bubbles (cavitation) could be observed at the removal interface (supplementary Video S1). Larger, stable bubbles were also observed in some recordings, which were found to negatively influence the hydrogel removal rate (Fig. 3).

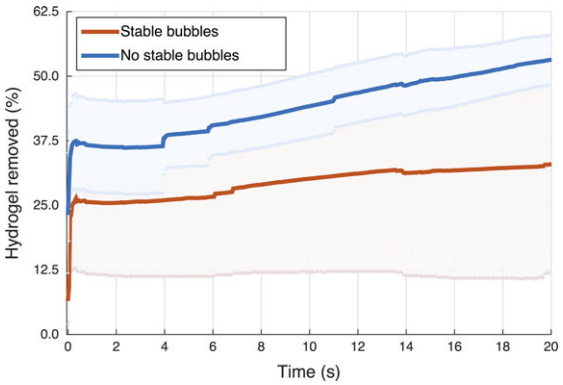

Figure 3 Hydrogel removal versus time in the presence or absence of bubbles.

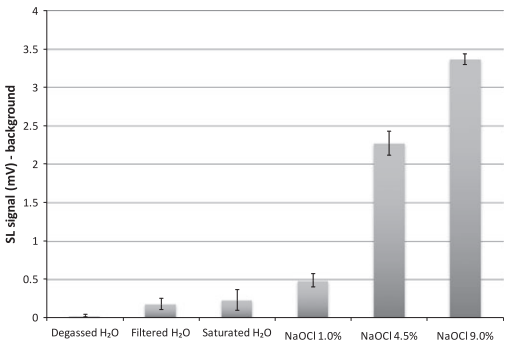

Figure 4 Sonoluminescence signal (background subtracted), representing the amount of cavitation, for various liquids. Error bars denote standard deviation.

Cavitation quantification

The SL intensity generated by IrriSafe 25 mm length, size 25 files in the six irrigant solutions is plotted in Fig. 4. It is evident that cavitation did not occur in degassed water with no difference with the background noise ($P = 0.597$). There was no significant difference in the SL value between the tap water regular and oversaturated water ($P = 0.538$), although their SL values were both higher than those for degassed water ($P < 0.043$). The highest SL signal was generated with NaOCl solutions ($P < 0.007$), which increased with concentration ($P < 0.014$).

Streaming

The flow pattern in the main root canal was similar to the flow patterns reported previously (Verhaagen *et al.* 2013a), showing oscillatory streaming in phase with the file oscillation; the steady streaming was shaped as

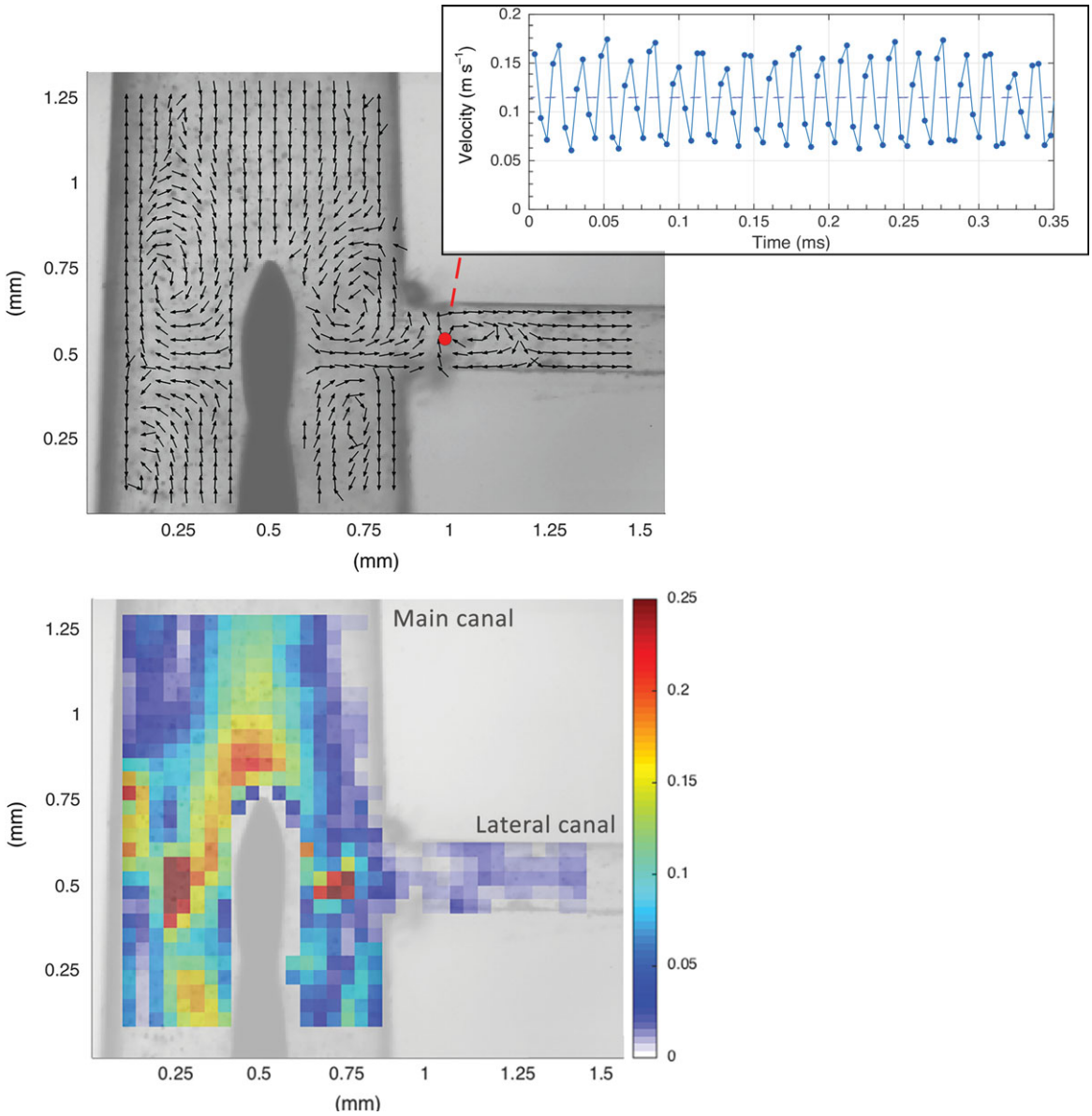

Figure 5 Example of an averaged PIV result near the tip of a *K*-file next to a lateral canal. The figure shows (top) the velocity vectors and (bottom) the velocity magnitude (m s^{-1}). The inset shows the oscillatory velocity at the indicated location inside the lateral canal, demonstrating the 30 kHz oscillation of the liquid. The average (steady) velocity is indicated with a dashed line.

jets occurring sideways from the file tip (Fig. 5). In the lateral canal, up to two vortices could be identified, driven by the jets (Verhaagen *et al.* 2013b). No qualitative differences were observed between the IrriSafe file and *K*-file and between the three liquids.

The steady (time-averaged) velocities decrease from approximately 0.3 m s^{-1} to below 0.05 m s^{-1} following penetration of 300 μm into the lateral canal (Fig. 6). The IrriSafe outperformed the *K*-file in fluid velocities in the lateral canal both at 3 and 6 mm (Fig. 6a vs. b). The velocities were higher in the lateral canal at 3 mm than at 6 mm (Fig. 6a vs. c). The differences between the three irrigants, however, were not significant.

The oscillatory component of the velocity shows the 30 kHz oscillation of the liquid (Fig. 5 inset), with rms velocities decreasing from approximately 0.5 m s^{-1} to below 0.1 m s^{-1} 450 μm into the lateral canal (Fig. 7).

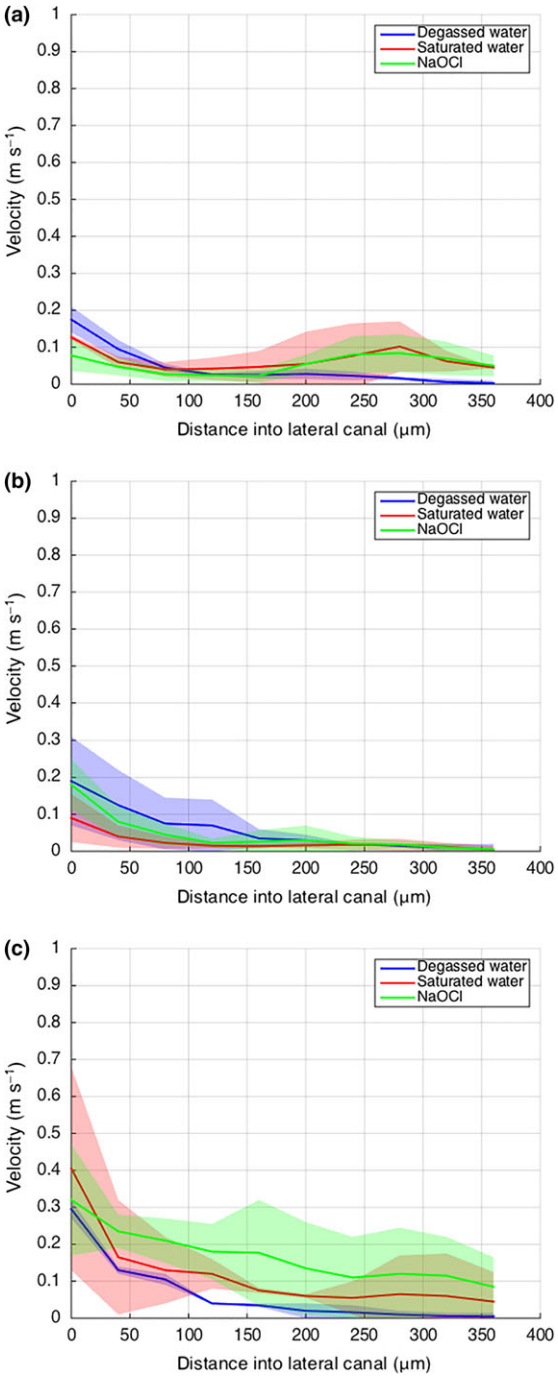

Figure 6 Steady velocity magnitudes as a function of distance within the lateral canal and for three different liquids. (a) *K*-file, lateral canal at 6 mm. (b) IrriSafe file, lateral canal at 6 mm. (c) *K*-file, lateral canal at 3 mm.

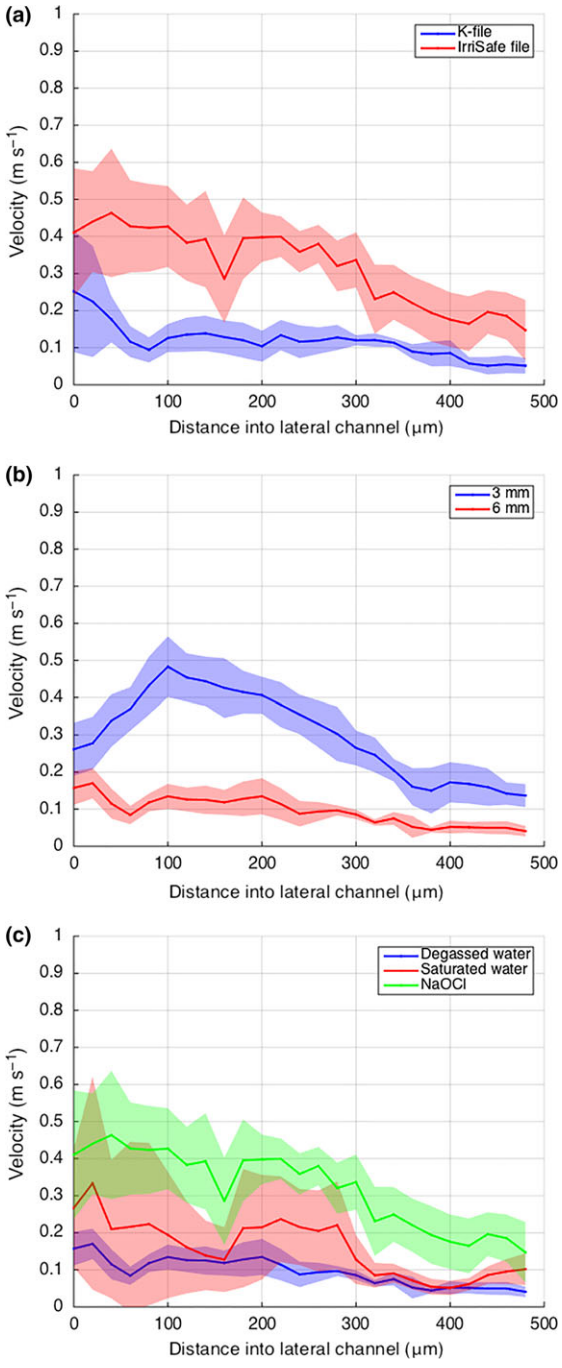

Figure 7 Rms oscillatory velocities within the lateral canal showing both the mean (solid lines) and standard deviations (shaded areas). (a) Comparison of the two file types, using NaOCl and the lateral canal at 6 mm. (b) Comparison of the lateral canal at two different positions, using degassed water and the IrriSafe file. (c) Comparison of the three liquids, using the IrriSafe file and the lateral canal at 6 mm.

The IrriSafe file outperformed the *K*-file when using saturated water or NaOCl; with degassed water, no significant differences were found. The oscillatory velocities

were higher inside the lateral canal at 3 mm compared to that at 6 mm. Velocities were found to be higher for NaOCl than that for saturated water, which was in turn higher than that for degassed water; this effect was present with both files and most prominent with the lateral canal at 6 mm. This measurement was repeated twice and in separate laboratories where the above findings were confirmed. The contribution of alignment or intermittent transient cavitation on the file tip to the streaming was therefore ruled out.

Discussion

A number of studies have shown that ultrasonic activation of the irrigant has yielded an improved outcome over syringe irrigation in cleaning isthmuses and irregularities in the canal wall (Lee *et al.* 2004, Gutarts *et al.* 2005, Rödig *et al.* 2010, Paque *et al.* 2011). Both streaming and cavitation have been proposed to play a significant role in the cleaning process (van der Sluis *et al.* 2007). This study measured both the amount of cavitation and the streaming in relation to the removal of a biofilm-mimicking hydrogel. Up to 64% of the hydrogel could be removed from a lateral canal within a time span of 20 s. The rate of hydrogel removal decreased as hydrogel removal progressed into the lateral canal. Simultaneously, the flow velocities of the vortices in the lateral canal decreased with distance into the lateral canal.

The IrriSafe file outperformed the *K*-file in removing the hydrogel from the lateral canal, for all irrigants and lateral canal positions. It has previously been shown that there is a greater amount of cavitation around an IrriSafe file than a *K*-file (Macedo *et al.* 2014a). Additionally, the IrriSafe file has a larger cross-section, leading to a closer proximity of the file to the root canal walls. It has also been demonstrated before that this can lead to higher velocities, as well as to an increased pressure and higher shear stresses; all aspects are beneficial for cleaning (Verhaagen *et al.* 2013a). These findings reject the null hypothesis.

The experimental data show that cleaning a lateral canal takes place even when using degassed water alone, in which, according to the sonochemiluminescence data, little (if any) cavitation occurs since degassing causes a reduction of the nuclei available for cavitation generation (Brennen 1995). This indicates that streaming around the files plays a significant role in hydrogel removal.

The cleaning rate was increased when NaOCl or oversaturated water was used instead of degassed water. This may have resulted from their increased gas content and/or the microbubble-stabilizing surfactant action of salts in NaOCl (Wall *et al.* 1999). The increased amount of cavitation in NaOCl and saturated water may initially appear as the cause leading to improved cleaning, especially as the streaming is assumed to be equal as the fluidic properties differ minimally between the liquids. However, the measurements revealed significant differences in fluid velocities in the three different liquids. The oscillatory component of the velocities was found to increase when using NaOCl compared with saturated or degassed water (in that order); no significant differences were found for the steady flow component. This finding for oscillatory velocity was unexpected as the acoustic streaming theory predicts that the oscillatory part of the flow is dominated by potential flow, which is independent of the fluidic properties. Possibly the small differences in fluidic properties (van der Sluis *et al.* 2010) have an effect on file oscillation and/or acoustic streaming effects. The effect of misalignment with respect to the lateral canal was ruled out by repeating experiments in different laboratories and by repositioning the file prior to experimental analysis. This approach should have eliminated variations in the alignment. 2D numerical simulations (Verhaagen *et al.* 2013a) using a model including a lateral canal also suggested that the file-to-canal alignment could not have led to this difference (C. Boutsioukis, B. Verhaagen, R. Macedo, L. van der Sluis, M. Versluis, unpublished data). Additionally, the effect of cavitation on the streaming was eliminated through additional repeats of the PIV experiments at different settings. Further research on these intriguing aspects is, therefore, needed.

In all the measurements involving the lateral canal at 6 mm from WL, significantly more hydrogel was removed with NaOCl as the irrigant; both the chemical dissolution potential and the effect on bubble formation are potential contributors and depend on the concentration of NaOCl. This finding is in line with previous studies (van der Sluis *et al.* 2010), but contrary to that of a previous report (Macedo *et al.* 2014c), which observed greater cleaning with water than with NaOCl. However, in that study, the lateral canal was located at the 3 mm position, and a greater concentration of NaOCl was used, both variables may, therefore, have resulted in greater amounts of inhibiting bubbles. To ensure reproducibility of the present set of experiments, the root canal models were ensured to be absent of large, stable air bubbles prior to cleaning.

With the lateral canal 3 mm from WL, more stable bubbles were formed that hindered hydrogel removal, see Fig. 3. This outcome could be due to the reduced confinement and closer file proximity to the root canal walls, leading to the higher velocities measured, as well as increased pressures and shear stresses (Verhaagen *et al.* 2012). Higher pressures may have also increased the probability of stable bubble formation. Previous studies observing this phenomenon suggest that the bubbles could be generated by rectified diffusion that is enhanced at higher acoustic pressures (Crum 1980, Macedo *et al.* 2014c). On the other hand, higher acoustic pressures that are generated in smaller confinements may result in greater forces being exerted on the hydrogel (as long as compressible bubbles are absent).

The set-up used in this study is an idealized situation that is useful for studying the effect of individual parameters such as file type, irrigant, and amount of cavitation and streaming on hydrogel removal. In practice, there may be several factors that affect the cleaning of a root canal. For example, whereas contact with the wall was avoided in the present set-up, it is very likely in narrow root canal preparations for the file to contact the root canal wall during activation, which has been shown to affect file oscillation and therefore streaming and cavitation (Boutsioukis *et al.* 2013a). Local complex root canal and lateral canal geometry may further complicate the streaming and therefore the cleaning by ultrasonic activation. Additionally, during clinical practice, the irrigant will not be as clean as used in this study but will contain debris and other contaminants that may affect the streaming, cavitation process and cleaning rate.

Furthermore, in the clinical situation, stable bubbles may enter into lateral canals prohibiting efficient cleaning, similar to a bubble being entrapped near the apex (vapour lock) (Boutsioukis *et al.* 2013b). Whilst a vapour lock can be removed with minimal effort (Boutsioukis *et al.* 2013b) a bubble within a lateral canal will be more difficult to remove due to its location. The clinical significance of the inhibiting stable bubbles should be investigated, and the conditions for formation of these bubbles and ways to remove them should be considered in future work.

Conclusions

The removal of a biofilm-mimicking hydrogel from a lateral canal by Ultrasonically Activated Irrigation was shown with up to 64% of the hydrogel removed within 20 s. Measurements of cavitation and acoustic streaming have provided insight into their contribution to cleaning. Significant differences in cleaning, cavitation and streaming were found depending on the file size, lateral canal location and irrigant used. In general, the IrriSafe file outperformed the *K*-file, and NaOCl was more effective than the other irrigants tested. The cavitation and streaming measurements showed that both contributed to the hydrogel removal and indicated that both play a significant role in root canal cleaning.

Acknowledgements

Jonathan Robinson gratefully acknowledges financial support from the EPSRC through a studentship from the PSIBS Doctoral Training Centre (EP/F50053X/1). He also would like to thank the EPSRC Engineering Instrument Pool for the loan of the high-speed camera used in the UK laboratory. This study was partly funded through grants of the Technology Foundation STW of the Netherlands. We thank Christos Boutsioukis (ACTA) for performing the 2D numerical simulations to study microstreaming and the effect of file-to-canal alignment. We also acknowledge the loan of equipment from the Optical Sciences group (University of Twente).

Conflict of interest

The other authors have stated explicitly that there are no conflict of interests in connection with this article.

References

Boutsioukis C, Verhaagen B, Walmsley AD, Versluis M, Van der Sluis LWM (2013a) Measurement and visualization of file-to-wall contact during ultrasonically activated irrigation in simulated canals. *International Endodontic Journal* **46**, 1046–55.

Boutsioukis C, Kastrinakis E, Lambrianidis T, Verhaagen B, Versluis M, van der Sluis LW (2013b) Formation and removal of apical vapor lock during syringe irrigation: a combined experimental and Computational Fluid Dynamics approach. *International Endodontic Journal* **47**, 191–201.

Brennen CE (1995) *Cavitation and Bubble Dynamics*. New York; Oxford: Oxford University Press.

Busscher HJ, Jager D, Finger G, Schaefer N, van der Mei HC (2010) Energy transfer, volumetric expansion, and removal of oral biofilms by non-contact brushing. *European Journal of Oral Science* **118**, 177–82.

Crum LA (1980) Measurements of the growth of air bubbles by rectified diffusion. *Journal of the Acoustical Society of America* **68**, 203–11.

Gutarts R, Nusstein J, Reader A, Beck M (2005) In vivo debridement efficacy of ultrasonic irrigation following hand-rotary instrumentation in human mandibular molars. *Journal of Endododontics* **31**, 166–70.

Köstgens V, Flemming H-C, Wingender J, Borchard W (2001) Uniaxial compression measurement device for investigation of the mechanical stability of biofilms. *Journal of Microbiological Methods* **46**, 9–17.

Lee SJ, Wu MK, Wesselink PR (2004) The effectiveness of syringe irrigation and ultrasonics to remove debris from simulated irregularities within prepared root canal walls. *International Endodontic Journal* **37**, 672–8.

Macedo RG, Verhaagen B, Fernandez Rivas D *et al.* (2014a) Sonochemical and high-speed optical characterization of cavitation generated by an ultrasonically oscillating dental file in root canal models. *Ultrasonics Sonochemistry* **21**, 324–35.

Macedo RG, Verhaagen B, Fernandez Rivas D, Wesselink PR, Versluis M, van der Sluis LWM (2014b) Cavitation measurement during sonically and ultrasonically activated irrigation. *Journal of Endodontics* **40**, 580–3.

Macedo RG, Robinson J, Verhaagen B *et al.* (2014c) A novel optical methodology for quantifying the removal of a biofilm-mimicking hydrogel from lateral morphological features of the root canal. *International Endodontic Journal* **47**, 1040–51.

Macedo RG, Verhaagen B, Wesselink PR, Versluis M, van der Sluis LWM (2014d) Influence of refreshment/activation cycles and temperature rise on the reaction rate of sodium hypochlorite with bovine dentine during ultrasonic activated irrigation. *International Endodontic Journal* **47**, 147–54.

Ohsumi T, Takenaka S, Wakamatsu R *et al.* (2015) Residual structure of Streptococcus mutans biofilm following complete disinfection favors secondary bacterial adhesion and biofilm re-development. *PLoS ONE* **10**, e0116647.

Paque F, Boessler C, Zehnder M (2011) Accumulated hard tissue debris levels in mesial roots of mandibular molars after sequential irrigation steps. *International Endodontic Journal* **44**, 148–53.

de Paz LC (2007) Redefining the persistent infection in root canals: possible role of biofilm communities. *Journal of Endodontics* **33**, 652–62.

Peters O, Schönenberger K, Laib A (2001) Effects of four Ni–Ti preparation techniques on root canal geometry assessed by micro computed tomography. *International Endodontic Journal* **34**, 221–30.

Ricucci D, Loghin S, Siqueira JF Jr (2013) Exuberant biofilm infection in a lateral canal as the cause of shortterm endodontic treatment failure: report of a case. *Journal of Endodontics* **39**, 712–8.

Rödig T, Bozkurt M, Konietschke F, Hülsmann M (2010) Comparison of the vibringe system with syringe and passive ultrasonic irrigation in removing debris from simulated root canal irregularities. *Journal of Endododontics* **36**, 1410–3.

van der Sluis LW, Versluis M, Wu MK, Wesselink PR (2007) Passive ultrasonic irrigation of the root canal: a review of the literature. *International Endodontic Journal* **40**, 415–26.

van der Sluis LWM, Vogels MPJM, Verhaagen B, Macedo R, Wesselink PR (2010) Study on the influence of refreshment/activation cycles and irrigants on mechanical cleaning efficiency during ultrasonic activation of the irrigant. *Journal of Endodontics* **36**, 737–40.

van der Sluis L, Boutsioukis C, Verhaagen B, Macedo RG, Jiang L, Versluis M (2015) Root canal irrigation. In: Sedgley C, Kishen A, Chaves de Paz L, eds. *The Endodontic Biofilm*, 1st edn. Berlin-Heidelberg, Germany: Springer Verlag.

Stewart PS, Franklin MJ (2008) Physiological heterogeneity in biofilms. *Nature Reviews Microbiology* **6**, 199–210.

Verhaagen B, Boutsioukis C, Heijnen G, van der Sluis L, Versluis M (2012) Role of the confinement of a root canal on jet impingement during endodontic irrigation. *Experiments in Fluids* **53**, 1841–53.

Verhaagen B, Boutsioukis C, van der Sluis LWM, Versluis M (2013a) Acoustic streaming induced by an ultrasonically oscillating endodontic file. *Journal of the Acoustical Society of America* **135**, 1717–30.

Verhaagen B, Boutsioukis C, Sleutel CP, Kastrinakis E, Versluis M, Van der Sluis LWM (2013b) Irrigant transport into dental microchannels. *Microfluidics and Nanofluidics* **16**, 1165–77.

Vogel AI (1962) *A Textbook of Quantitative Inorganic Analysis*, 3rd edn, 2nd impression, London, UK: Longmans, pp. 363–5.

Wall M, Ashokkumar M, Tronson R, Grieser F (1999) Multibubble sonoluminescence in aqueous salt solutions. *Ultrasonics Sonochemistry* **6**, 7–14.

Wu MK, Wesselink PR (2005) Timeliness and effectiveness in the surgical management of persistent posttreatment periapical pathosis. *Endodontic Topics* **11**, 25–31.

Supporting Information

Additional Supporting Information may be found in the online version of this article:

Video S1. Observation of bubbles (small black shapes) at the interface of the hydrogel (blue) during activation of the file (black moving shape) inside a root canal model.

